

Elucidation of a Sc(I) Complex by DFT Calculations and Reactivity Studies<sup>†</sup>

Ana-Mirela Neculai, Christopher C. Cummins, Dante Neculai, Herbert W. Roesky,\* Gábor Bunkóczi, Bernhardt Walfort, and Dietmar Stalke

Institut für Anorganische Chemie, Universität Göttingen, Tammannstrasse 4, D-37077 Göttingen, Germany, Institut für Anorganische Chemie, Am Hubland, D-97074 Würzburg, Germany, and Department of Chemistry Room 2-227, Massachusetts Institute of Technology, Cambridge, Massachusetts 02139-4307

Received August 8, 2003

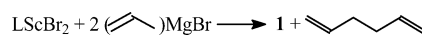
Sc(BrMgL)<sub>2</sub>Br (L = (R<sub>2</sub>NCH<sub>2</sub>CH<sub>2</sub>NCMe)<sub>2</sub>CH, R = H) was studied by DFT methods leading to the conclusion that this diamagnetic formal scandium(I) system enjoys stabilization of its Sc-based filled d<sub>yz</sub> orbital by a δ-acceptor linear combination of BrMgL ring orbitals. Investigation of the reactivity of Sc(BrMgL)<sub>2</sub>Br (L = (R<sub>2</sub>NCH<sub>2</sub>CH<sub>2</sub>NCMe)<sub>2</sub>CH, R = Et) with H<sub>2</sub>O·B(C<sub>6</sub>F<sub>5</sub>)<sub>3</sub> and (HOCH<sub>2</sub>)<sub>2</sub>CMe<sub>2</sub>, respectively, led to decomposition, with LMgBr being isolated in the latter case.

## Introduction

In the organometallic chemistry of the lanthanides, molecular complexes incorporating low-oxidation-state metals hold a particular interest. The availability of compounds with the formal oxidation state +2 for samarium, europium, and ytterbium due to the stability of the f<sup>6</sup>, f<sup>7</sup>, and f<sup>14</sup> electronic configurations is no longer a problem.<sup>1</sup> In recent years, reports on lanthanum and scandium increased the number of the rare earth +2 compounds.<sup>2–4</sup> In most of the metal (0) or (+1) containing compounds, stabilization is ensured by using a considerably bulky ligand with π-acceptor properties<sup>5</sup> that supports back-donation of electron density from the metal.

Incontestably, the principally used technique for accessing low oxidation states in different ligand environments for these metals apart from samarium, europium, and ytterbium is metal vapor synthesis.<sup>5</sup> Our recent interest in the chemistry of β-diketiminato derivatives of scandium<sup>6</sup> led us to an unexpected sandwich-like scandium (+1) complex (Scheme 1 and Figure 1).<sup>7</sup>

## Scheme 1



In comparison with the first reported Sc(I) compound,<sup>3</sup> this complex is obtained in a facile route in solution, and it is diamagnetic. Earlier this year another subvalent scandium compound with a 1,2,4-triphosphacyclopentadienyl ligand, [Sc{(P<sub>3</sub>C<sub>2</sub>tBu)<sub>2</sub>}<sub>2</sub>], was reported by Cloke and co-workers.<sup>4</sup> This compound presented as a mixed valence dimer Sc(I)–Sc(III) displaying a magnetic behavior similar to that of **1**. A reasonable extension of our work is the investigation through calculations on the basis of the unusual magnetic behavior of compound **1** and the investigation of the reactivity of such a scandium +1 center. In this paper, we describe the outcome of the theoretical study and the results of redox reactions undergone by **1** with H<sub>2</sub>O·B(C<sub>6</sub>F<sub>5</sub>)<sub>3</sub> and (HOCH<sub>2</sub>)<sub>2</sub>CMe<sub>2</sub>. This work is designed to shed light on the

\* To whom correspondence should be addressed. E-mail: hroesky@gwdg.de. Phone: +49-551-393001. Fax: +49-551-393373.

<sup>†</sup> Dedicated to Professor Reinhard Schmutzler on the occasion of his 70th birthday.

- (1) (a) Huheey, J. E.; Keiter, E. A.; Keiter, R. L. *Inorganic Chemistry: Principles of Structure and Reactivity*, 4th ed.; Harper Collins College Publishers: New York, 1993; pp 509–602. (b) Cotton, F. A.; Wilkinson, E.; Murillo, C. A.; Bochmann, M. *Advanced Inorganic Chemistry*, 6th ed.; John Wiley & Sons: New York, 1999; p 1127. (c) Avent, A. G.; Khvostov, A. V.; Hitchcock, P. B.; Lappert, M. F. *Chem. Commun.* **2002**, 1410–1411.
- (2) Cassani, M. C.; Duncalf, D. J.; Lappert, F. M. *J. Am. Chem. Soc.* **1998**, *120*, 12958–12959.
- (3) Arnold, L. P.; Cloke, F. G. N.; Hitchcock, P. B.; Nixon, J. F. *J. Am. Chem. Soc.* **1996**, *118*, 7630–7631.
- (4) Clentsmith, G. K. B.; Cloke, F. G. N.; Green, J. C.; Hanks, J.; Hitchcock, P. B.; Nixon, J. F. *Angew. Chem.* **2003**, *115*, 1068–1069; *Angew. Chem., Int. Ed.* **2003**, *42*, 1038–1039.
- (5) (a) Cloke, F. G. N. *Chem. Soc. Rev.* **1993**, 17–24 and references therein. (b) Arnold, P. L.; Cloke, F. G. N. *Chem. Commun.* **1997**, 481–482.

(6) Neculai, A. M.; Roesky, H. W.; Neculai, D.; Magull, J. *Organometallics* **2001**, *26*, 5501–5503.

(7) Neculai, A. M.; Neculai, D.; Roesky, H. W.; Magull, J.; Baldus, M.; Andronesi, O.; Jansen, M. *Organometallics* **2002**, *21*, 2590–2592.

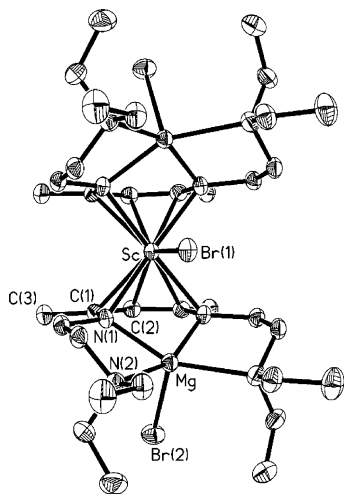


**Figure 1.** Molecular structure of **1**. Solvent and protons are omitted for clarity.

question of the best formal oxidation state assignment for the scandium center in complex **1**.

## Experimental Section

**General Comments.** All manipulations were performed on a high-vacuum line or in a glovebox under a purified  $N_2$  atmosphere, using Schlenk techniques with rigorous exclusion of moisture and air. All the necessary glassware was oven-dried at  $150\text{ }^\circ\text{C}$  for a minimum period of 12 h, assembled hot, and cooled under high vacuum with intermittent flushing of nitrogen or argon. The samples for spectral measurements were prepared inside a MBraun MB 150-GI glovebox where the  $O_2$  and  $H_2O$  levels were normally maintained below 1 ppm. Toluene was distilled from Na/benzophenone, THF from Na prior to use. The melting points of **1**, **2**, and **3** were measured in sealed capillaries on a Bühler SPA-1 instrument.

$^1\text{H}$ ,  $^{13}\text{C}$ , and  $^{45}\text{Sc}$  NMR spectra (benzene- $d_6$ , THF- $d_8$ , toluene- $d_8$ ) were recorded on Bruker MSL-400, AM-250, and AM-200 instruments. Solid-state  $^{45}\text{Sc}$  and  $^{13}\text{C}$  NMR spectra were recorded on Bruker A-600. The solvents for NMR measurements were dried over K or  $\text{CaH}_2$  and trap-to-trap distilled prior to use. Mass spectra were obtained on a Finnigan MAT 8230 by EI technique. EPR spectra were recorded on a Varian Century-Line 9 GHz. UV–vis spectrum was recorded on a Perkin-Elmer 320. Magnetic measurements were performed on a Squid-Magnetometer (Quantum Design, California) at different magnetic fields in the range of temperatures between 2 and 300 K.

**Reaction of **1** with  $\text{H}_2\text{O}\cdot\text{B}(\text{C}_6\text{F}_5)_3$ .** A 0.1 g (1.8 mmol) portion of  $\text{H}_2\text{O}\cdot\text{B}(\text{C}_6\text{F}_5)_3$  was added to a solution of 0.075 g (0.07 mmol) of **1** (obtained from reaction of 0.3 g (0.6 mmol) of  $\text{LScBr}_2$  with 1.2 mL of  $(\text{C}_3\text{H}_5)\text{MgBr}$  (1 M in ether, 1.2 mmol) in a yield of 25%) in toluene (10 mL). The reaction mixture immediately turned to brown. After stirring for a further hour, the solution was concentrated to approx 5 mL until it became turbid and 5 mL THF was added to dissolve the precipitate. Colorless crystals of **2** suitable for X-ray analyses appeared after one week at  $-26\text{ }^\circ\text{C}$  (approx 0.050 g). Mp  $167\text{--}178\text{ }^\circ\text{C}$ . Anal. Calcd for  $\text{C}_{41}\text{H}_{35}\text{N}_4\text{B}_2\text{F}_{20}\text{O}_2\text{Sc}$ : C, 46.36; H, 3.32; N, 5.27. Found: C, 46.86; H, 3.98; N, 5.06.  $^1\text{H}$  NMR (500 MHz,  $\text{C}_6\text{D}_6$ , 300 K):  $\delta = 3.51$  (s, 1 H,  $\text{C}(\text{Me})\text{CHC}(\text{Me})$ ), 2.96 (t, 4 H;  $\text{Et}_2\text{NCH}_2\text{CH}_2$ ), 2.75 (m, 8 H,  $\text{NCH}_2\text{CH}_3$ ), 2.58 (t, 4 H,  $\text{Et}_2\text{NCH}_2\text{CH}_2$ ), 1.40 (s, 6H,  $\text{CCH}_3$ ), 0.72 (t,  $\text{NCH}_2\text{CH}_3$ ).  $^{19}\text{F}$  NMR (188 MHz, ext  $\text{C}_6\text{F}_6$ ,  $\text{C}_6\text{D}_6$ , 300 K):  $-136.7$  (q, 8F,  $\text{BC}_6\text{F}_5$  ortho),  $-155.8$  (t, 4F,  $\text{BC}_6\text{F}_5$  para),  $-162.7$  (m, 8F,  $\text{BC}_6\text{F}_5$  meta).  $^{45}\text{Sc}$  NMR (121 MHz, referenced to  $[\text{Sc}(\text{H}_2\text{O})_6]^{3+}$  in  $\text{D}_2\text{O}$ ,  $\text{C}_6\text{D}_6$ ,

300 K):  $\delta 244.11$ . EI-MS:  $m/z$  (rel int %) 1062 [ $\text{C}_{41}\text{H}_{35}\text{N}_4\text{B}_2\text{F}_{20}\text{O}_2\text{Sc}^+$ , 5], 976 [ $\text{C}_{41}\text{H}_{35}\text{N}_4\text{B}_2\text{F}_{20}\text{O}_2\text{Sc}^+ - \text{C}_5\text{H}_{12}\text{N}$ , 50], 86 [ $\text{C}_5\text{H}_{12}\text{N}$ , 100].

**Reaction of **1** with  $(\text{HOCH}_2)_2\text{CMe}_2$ .** A solution of 0.125 g of  $(\text{HOCH}_2)_2\text{CMe}_2$  (2 mmol) in toluene (5 mL) was added to a solution of **1** (obtained from reaction of 0.5 g (1 mmol) of  $\text{LScBr}_2$  with 2 mL of  $(\text{C}_3\text{H}_5)\text{MgBr}$  (1 M in ether, 2 mmol) of a yield of 25%) in toluene (15 mL). The reaction takes place instantaneously with formation of a brown solution that was stirred for 6 h which was then concentrated to approx 10 mL, and 1 mL THF was added. Crystals of **3** were obtained after several days at  $-26\text{ }^\circ\text{C}$ .

The reaction was repeated in a NMR tube with 0.020 g of **1** (0.02 mmol) in  $\text{C}_6\text{D}_6$  (0.5 mL) and 0.002 g of  $(\text{HOCH}_2)_2\text{CMe}_2$  in  $\text{C}_6\text{D}_6$  (0.5 mL). The  $^1\text{H}$  NMR spectrum was recorded after 5 min and 24 h. The second  $^1\text{H}$  NMR spectrum showed no changes in comparison with the first one. Spectral data for **3** follow.  $^1\text{H}$  NMR (500 MHz,  $\text{C}_6\text{D}_6$ , 300 K):  $\delta 4.74$  (s, 2 H,  $\text{C}(\text{Me})\text{CHC}(\text{Me})$ ), 3.62 and 2.63 br signals assigned to 16H,  $\text{CH}_2$ , 1.80 (s, 6 H,  $\text{CCH}_3$ ), 0.72 (t, 24 H,  $\text{NCH}_2\text{CH}_3$ ).

**X-ray Crystallography.** Data for the crystal structure of **1**-toluene were collected on a Stoe Image Plate IPDS II-System, for **2** on a Stoe-Siemens-Huber four circle diffractometer, and for **3** on Bruker Smart Apex CCD diffractometer. For refinement of **2** and **3** as nonmerohedric twins, the two matrices of the two domains were determined, and every domain was integrated on its own. Then a new file with the reflections of the dominant domain was written, without reflections that were strongly overlapped with reflections of the other domain. With these data, the structures were solved and refined.

The structures were solved by direct methods (SHELX-97) and refined against  $F^2$  using SHELXL-97.<sup>8</sup>  $R$  values were defined as  $R1 = \sum||F_o| - |F_c||/\sum|F_o|$ ,  $wR2 = [\sum w(F_o^2 - F_c^2)^2/\sum w(F_o^2)^2]^{0.5}$ ,  $w = [\sigma^2(F_o^2) + (g_1P)^2 + g_2P]^{-1}$ ,  $P = 1/3[\max(F_o^2, 0) + 2F_c^2]$ . Heavy atoms were refined anisotropically. Hydrogen atoms were included using the riding model with  $U_{\text{iso}}$  tied to  $U_{\text{iso}}$  of the parent atoms. Crystal data collection details, and the solution and refinement procedures, are summarized in Table 1.

**Theoretical Calculations.** NMR shielding calculations for complexes **1** and  $\text{Cp}_2\text{Sc}(\text{BH}_4)^9$  were carried out using density functional theory (DFT) and gauge-including atomic orbitals (GIAOs) using the Amsterdam Density Functional package (version *ADF2000.02*).<sup>10</sup> The method involved has been described in detail by Schreckenbach in his description of the  $^{57}\text{Fe}$  NMR shieldings in ferrocene.<sup>11</sup> For the purpose of minimizing the calculation time, the model system  $\text{Sc}(\text{BrMgL})_2\text{Br}$  ( $\text{L} = (\text{R}_2\text{NCH}_2\text{CH}_2\text{NCMe})_2\text{CH}$ ,  $\text{R} = \text{H}$ ) was used where ethyl groups remote from scandium in the real system are replaced by hydrogen atoms. The remainder of the molecule was left intact. Since the real system is known to crystallize with  $C_{2v}$  molecular point group symmetry, geometry

- (8) (a) Sheldrick, G. M. *Acta Crystallogr., Sect. A* **1990**, *46*, 467–473. (b) Sheldrick, G. M. *SHELXL-97, Program for Crystal Structure Refinement*; University of Göttingen: Göttingen, Germany, 1997.
- (9) (a) Schreckenbach, G.; Ziegler, T. *J. Phys. Chem.* **1995**, *99*, 606–611. (b) Schreckenbach, G.; Ziegler, T. *Int. J. Quantum Chem.* **1996**, *60*, 753–766. (c) Schreckenbach, G.; Ziegler, T. *Int. J. Quantum Chem.* **1997**, *61*, 899–918. (d) Wolff, S. K.; Ziegler, T. *J. Chem. Phys.* **1998**, *109*, 895–905. (e) Wolff, S.; Ziegler, K. T.; van Lenthe, E.; Baerends, E. J. *J. Chem. Phys.* **1999**, *110*, 7689–7698. (f) Gilbert, T. M.; Ziegler, T. *J. Phys. Chem. A* **1999**, *103*, 7535–7543.
- (10) (a) Baerends, E. J.; Ros, P. *Chem. Phys.* **1975**, *8*, 412–418. (b) Versluis, L.; Ziegler, T. *J. Chem. Phys.* **1988**, *88*, 322–328. (c) Velde, G. T.; Baerends, E. J. *J. Comput. Phys.* **1992**, *99*, 84–98. (d) Fonseca Guerra, C.; Snijders, J. G.; Velde, G. T.; Baerends, E. J. *Theor. Chem. Acc.* **1998**, *99*, 391–403.
- (11) Schreckenbach, G. *J. Chem. Phys.* **1999**, *110*, 11936–11949.

**Table 1.** Summary of Crystallographic Data

	1•toluene	2•toluene	3•0.5toluene
formula	C <sub>41</sub> H <sub>78</sub> Br <sub>3</sub> Mg <sub>2</sub> N <sub>8</sub> Sc	C <sub>48</sub> H <sub>43</sub> N <sub>4</sub> B <sub>2</sub> F <sub>20</sub> O <sub>2</sub> Sc	C <sub>20.50</sub> H <sub>39</sub> BrMgN <sub>4</sub>
fw	1016.42	1154.44	445.78
space group	<i>Cmcm</i>	<i>P1</i>	<i>P2<sub>1</sub>/c</i>
cryst syst	orthorhombic	triclinic	monoclinic
<i>a</i> , Å	21.5760(12)	10.865(2)	17.508(4) Å
<i>b</i> , Å	12.9704(7)	13.518(3)	7.2970(14)
<i>c</i> , Å	17.7340(8)	19.172(4)	19.674(4)
$\alpha$ , deg		71.83(3)	
$\beta$ , deg		85.12(3)	110.493(3)
$\gamma$ , deg		69.11(3)	
<i>V</i> , Å <sup>3</sup>	2148.51(17)	2498.6(9)	2354.4(8)
<i>Z</i>	4	2	4
<i>D</i> <sub>calcd.</sub> , g/cm <sup>3</sup>	1.360	1.534	1.258
temp, K	133(2)	133(2)	173(2)
2 $\theta$ range, deg	1.83–24.71	1.12–23.21	2.21–27.10
index ranges	–25 ≤ <i>h</i> ≤ 25 –15 ≤ <i>k</i> ≤ 14 –20 ≤ <i>l</i> ≤ 18	–11 ≤ <i>h</i> ≤ 12 –13 ≤ <i>k</i> ≤ 14 0 ≤ <i>l</i> ≤ 21	–22 ≤ <i>h</i> ≤ 21 0 ≤ <i>k</i> ≤ 9 0 ≤ <i>l</i> ≤ 25
reflns collected/unique	26177/2256 [ <i>R</i> (int) = 0.0720]	12159/12159 [ <i>R</i> (int) = 0.0000]	23318/5067 [ <i>R</i> (int) = 0.0768]
completeness to $\theta$ (%)	99.9	98.3	97.5
data/restraints/params	2256/0/199	12159/856/767	5067/0/266
GOF	1.107	1.080	1.052
final <i>R</i> indices [ <i>I</i> > 2 $\sigma$ ( <i>I</i> )]	<i>R</i> 1 = 0.0315, <i>wR</i> 2 = 0.0849	<i>R</i> 1 = 0.0454, <i>wR</i> 2 = 0.1364	<i>R</i> 1 = 0.0567, <i>wR</i> 2 = 0.1372
<i>R</i> indices (all data)	<i>R</i> 1 = 0.0346, <i>wR</i> 2 = 0.0867	<i>R</i> 1 = 0.0486, <i>wR</i> 2 = 0.1403	<i>R</i> 1 = 0.0874, <i>wR</i> 2 = 0.1570
largest diff peak and hole (e/Å <sup>3</sup> )	0.946 and –0.608	0.329 and –0.435	1.966 and –0.596

optimization on the model system was carried out with imposition of this symmetry constraint. Since no structural data are available for Cp<sub>2</sub>Sc(BH<sub>4</sub>), we carried out geometry optimization taking the  $\eta^3$ -BH<sub>4</sub> bonding mode as a starting point, employing no symmetry constraints. Since the Cp<sub>2</sub>Sc(BH<sub>4</sub>) system exhibited a tendency to C<sub>s</sub> symmetry, final optimization was carried out with incorporation of this constraint. Single-point calculations, preceding the NMR calculations, were run using the Zora(V) basis set for all atoms, as implemented in the ADF suite. Full electronic configuration was used for all atoms. Relativistic effects were included by virtue of the zero order regular approximation (ZORA).<sup>12</sup> However, no spin-orbit coupling effects were taken into account in the derivation of the isotropic shielding for the scandium atoms. The local density approximation (LDA) by Vosko, Wilk, and Nusair (VWN)<sup>13</sup> was used together with the exchange and correlation corrections published by Perdew in 1991 (PW91).<sup>14</sup>

## Results and Discussion

Our aforementioned work<sup>7</sup> formulated, accordingly to the X-ray and NMR studies, compound **1** as Sc(BrMgL)<sub>2</sub>Br (L = (R<sub>2</sub>NCH<sub>2</sub>CH<sub>2</sub>NCMe)<sub>2</sub>CH, R = Et). But magnetic and EPR measurements exposed an interesting and unanticipated magnetic behavior (diamagnetic) for the compound, a detailed understanding of which warranted a computational study as follows.

A DFT study performed on the model system Sc-(BrMgL)<sub>2</sub>Br (L = (R<sub>2</sub>NCH<sub>2</sub>CH<sub>2</sub>NCMe)<sub>2</sub>CH, R = H) re-

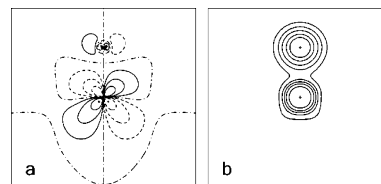


**Figure 2.** (a) A contour plot of the molecule's highest occupied molecular orbital (HOMO) in the *yz* plane, with Sc located at the origin. The Sc–Br vector defines the *z* axis (vertical) and the HOMO in the C<sub>2v</sub> point group has *b*<sub>2</sub> symmetry. (b) This shows the same 10 × 10 Å<sup>2</sup> area in the *yz* plane, but it displays contours corresponding to the total SCF electron density.

vealed that the HOMO (Figure 2a) is comprised largely of the scandium *d*<sub>*yz*</sub> orbital, which is antibonding with respect to the filled bromine *p*<sub>*y*</sub> orbital. Nodal surfaces cutting through the *yz* plane are indicated in Figure 2a by dash-dot-dash (–·–) lines, while solid (—) lines and dashes (– –) denote positive and negative contours, respectively.

From the standpoint of energy considerations, the HOMO is located nearly equidistant between the HOMO – 1 and LUMO orbitals, a characteristic typically identified with a nonbonding (lone pair) orbital (Figure 5). This is consistent with assigning a formal +1 oxidation state to the scandium center. Examination of the HOMO in three dimensions suggests a substantial stabilization by virtue of  $\delta$ -backbonding to the two heterocyclic rings sandwiching the scandium atom (Figure 3).

The bromine atom (top) and the scandium atom (bottom) are the only atoms that have significant electron density in the *yz* plane within this area.

Schreckenbach has elucidated the electronic mechanism of the <sup>57</sup>Fe NMR shielding in ferrocene and in iron pentacarbonyl.<sup>11</sup> He makes note that the diamagnetic contribution to the shielding,  $\sigma^d$ , does not contribute to relative chemical shifts because it is due to contributions from core

- (12) (a) Snijders, J. G.; Baerends, E. J.; Ros, P. *Mol. Phys.* **1979**, *38*, 1909–1929. (b) Ziegler, T.; Tschinke, V.; Baerends, E. J.; Snijders, J. G.; Ravenek, W. *J. Phys. Chem.* **1989**, *93*, 3050–3056. (c) van Lenthe, E.; Baerends, E. J.; Snijders, J. G. *J. Chem. Phys.* **1993**, *99*, 4597–4610.
- (13) Vosko, S. H.; Wilk, L.; Nusair, M. *Can. J. Phys.* **1980**, *58*, 1200–1211.
- (14) Perdew, J. P.; Chevary, J. A.; Vosko, S. H.; Jackson, K. A.; Pederson, M. R.; Singh, D. J.; Fiolhais, C. *Phys. Rev. B* **1992**, *46*, 6671–6687.

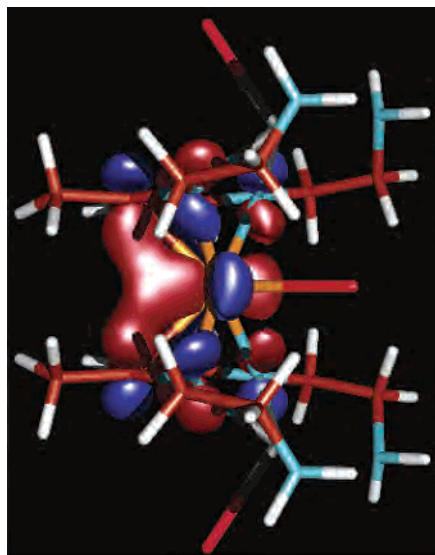


Figure 3. HOMO orbital of **1** in three dimensions.

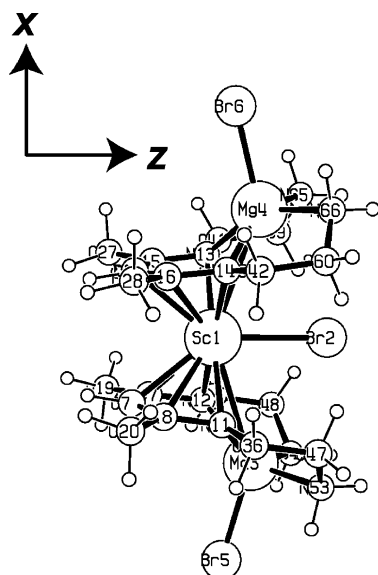


Figure 4. Calculated structure of the model compound  $\text{Sc}(\text{MgBrL})_2\text{Br}$ , where L is  $(\text{R}_2\text{NCH}_2\text{CH}_2\text{NCMe})_2\text{CH}$  with  $\text{R} = \text{H}$ . Shown also are the Cartesian axis directions used for the NMR calculation. The molecule is oriented with Sc at the origin, the Sc–Br2 vector defining the z axis, and the xz plane being a mirror plane containing Sc, the three bromine atoms, and the two Mg atoms. Selected bond distances (Å): Sc1–Br2, 2.799; Sc–N13, 2.319; Sc–C15, 2.494; Sc–C8, 2.510; Mg4–N13, 2.163; Mg4–Br6, 2.525; Sc1–Mg4, 3.276.

electrons and is thus essentially invariant from one compound to another. Further, Schreckenbach points out that this truism has been noted previously for a variety of nuclei. By far the greatest contributor to the total shielding, in the absence of large spin–orbit effects,<sup>15</sup> typically is the occupied–virtual component of the paramagnetic shielding term,  $\sigma^{p,oc-vir}$ . Additionally, it may turn out, as for the ferrocene <sup>57</sup>Fe case, that only a few occupied–virtual molecular orbital (MO) couplings determine the paramagnetic shielding almost completely. In such a case, the NMR shift and its associated anisotropy represent a sensitive probe of frontier MO

electronic structure. Herein we use Schreckenbach’s method to analyze via density functional theory (DFT) calculations the electronic structure of **1**. The major MO mixings contributing to  $\sigma^{p,oc-vir}$  are elucidated and are compared with those found for a reference scandium(III) sandwich system,  $\text{Cp}_2\text{Sc}(\text{BH}_4)$ .<sup>16</sup> Both systems have been studied by solution <sup>45</sup>Sc NMR methods,<sup>15,16</sup> and the present work suggests that it would be of interest to probe their predicted anisotropies by solid-state <sup>45</sup>Sc NMR techniques. A priori expectations for any scandium(I) system include a small HOMO–LUMO gap and therefore a strong downfield shift relative to scandium(III) systems. This is because the MO mixings that comprise  $\sigma^{p,oc-vir}$  become stronger as the gap between the involved orbitals diminishes. A small HOMO–LUMO gap is expected for scandium(I) because this oxidation state assignment implies a lone pair of electrons localized on scandium, i.e., a high-lying HOMO. To the extent that the HOMO becomes delocalized onto the ligands, the effect on the <sup>45</sup>Sc NMR downfield shift may be expected to diminish; Schreckenbach found that the most substantive MO mixings comprising  $\sigma^{p,oc-vir}$  for ferrocene are between MOs having substantial iron 3d character.<sup>11</sup> Calculations were carried out on the same model system  $\text{Sc}(\text{BrMgL})_2\text{Br}$  (L =  $(\text{R}_2\text{NCH}_2\text{CH}_2\text{NCMe})_2\text{CH}$ , R = H) where ethyl groups remote from scandium in the real system are replaced by hydrogen atoms (Figure 4).

Depicted in Figure 5a is a set of three energy level diagrams (corresponding to  $R_x$ ,  $R_y$ , and  $R_z$ ) for  $\text{Sc}(\text{BrMgL})_2\text{Br}$  indicating via vertical dashed lines the five strongest occupied–virtual MO couplings as a function, respectively, of the three Cartesian axis directions. Separation of the occupied–virtual MO couplings in this manner comes about because the magnetic operator has the same symmetry properties as the  $R_x$ ,  $R_y$ , and  $R_z$  rotations about the Cartesian axes. Note that the HOMO is, as anticipated for scandium(I), energetically high-lying.

In the point group  $C_{2v}$ , for example,  $R_x$  has  $B_2$  symmetry, and thus, the magnetic field can induce mixing about the x axis between occupied and virtual orbitals whose direct product is also of  $B_2$  symmetry. The strongest such MO mixing associated with  $R_x$  is accordingly seen to be between 37B2 (the HOMO) and 59A1 (the LUMO + 1). Associated with this pair of orbitals is a small energy gap and a  $B_2$  symmetric direct product. In contrast to the delocalization of the HOMO, the LUMO + 1 with which the HOMO may mix strongly via  $R_x$  is a nearly pure  $d_{x^2-y^2}$  orbital. From a physical point of view, in the presence of an applied magnetic field a current is induced about the x axis involving the lobes of scandium’s  $d_{yz}$  and  $d_{x^2-y^2}$  orbitals that reside in the yz plane. Even though the LUMO + 12 (64A1) is energetically well-separated from the HOMO, it is this orbital (scandium localized and of  $d_z^2$  symmetry) with which the HOMO couples second-strongest. It is worthwhile at this point to make mention of the calculated chemical shielding anisotropy associated with  $\text{Sc}(\text{BrMgL})_2\text{Br}$ . The Cartesian axes indicated

(15) Rodriguez-Fortea, A.; Alemany, P.; Ziegler, T. *J. Phys. Chem. A* **1999**, *103*, 8288–8294.

(16) Mancini, M.; Bougeard, P.; Burns, R. C.; Mlekuz, M.; Sayer, B. G.; Thompson, J. I. A.; McGlinchey, M. J. *Inorg. Chem.* **1984**, *23*, 1072–1078.

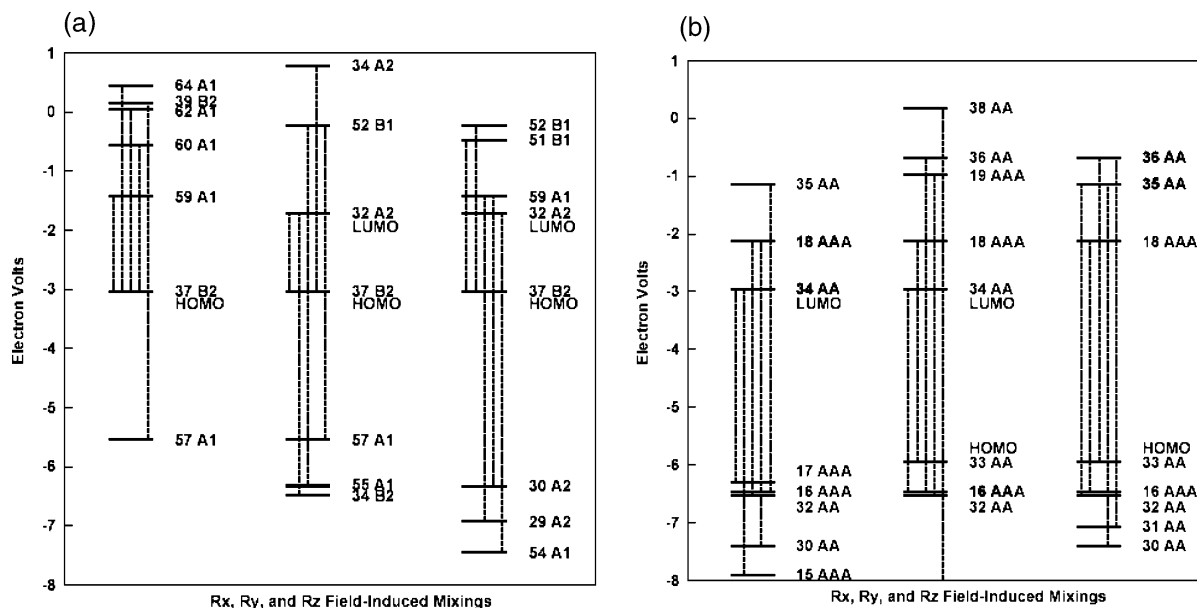


**Figure 5.** (a) Plot of the 5 strongest field-induced mixings of occupied and virtual energy levels of  $\text{Sc}(\text{MgBrL})_2\text{Br}$  for each of the three rotations  $R_x$ ,  $R_y$ , and  $R_z$ , from left to right (left side). (b) Plot of the 5 strongest field-induced mixings of occupied and virtual energy levels of  $\text{Cp}_2\text{ScBH}_4$  for each of the three rotations  $R_x$ ,  $R_y$ , and  $R_z$ , from left to right (right side).

in Figure 4 map onto the magnetic shielding in the following manner:  $x$ ,  $\delta_{11}$ ;  $y$ ,  $\delta_{33}$ ;  $z$ ,  $\delta_{22}$ . What this means is that the strongest  $\sigma^{\text{p,oc-vir}}$  and largest downfield chemical shifts are associated with the Cartesian  $x$  axis direction. The system is found to be rhombic; i.e.,  $\delta_{11} \neq \delta_{22} \neq \delta_{33}$ . The orbitals that are most strongly mixed by the  $R_y$  magnetic operator are 37B2 (HOMO) with 32A2 (LUMO), and the second being 34B2 (HOMO - 13) with 32A2 (LUMO), and by the  $R_z$  magnetic operator are 37B2 (HOMO) with 51B1 (LUMO + 3) and 37B2 (HOMO) with 52B1 (LUMO + 5), respectively. Note that although HOMO-LUMO mixing is facilitated by  $R_y$ , it is associated with  $\delta_{33}$  and the direction of weakest paramagnetic shielding. This is because the LUMO is mostly ligand-based with only a very small contribution from the scandium  $d_{xy}$  orbital. LUMO + 3 and LUMO + 5 both enjoy strong contributions from scandium's  $d_{xz}$  orbital, leading to the intermediate coupling and downfield shift associated with  $\delta_{22}$  and  $R_z$  (see Supporting Information).

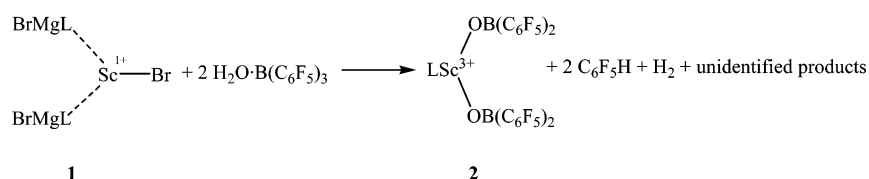
Now it is appropriate to ask if the calculated shieldings for  $\text{Sc}(\text{BrMgL})_2\text{Br}$  really do signify a downfield shift relative to a typical scandium(III) reference compound. For this purpose we choose  $\text{Cp}_2\text{Sc}(\text{BH}_4)$ , a sandwich complex geometrically similar to  $\text{Sc}(\text{BrMgL})_2\text{Br}$  but with what most would agree to be an unambiguous example of scandium in the +3 oxidation state.

McGlinchey and co-workers assigned to the borohydride ligand of  $\text{Cp}_2\text{Sc}(\text{BH}_4)$  an  $\eta^3$  bonding mode, despite the fact that their orbital analysis suggested  $\text{BH}_4^-$  to be only a 4e donor to the  $\text{Cp}_2\text{Sc}^+$  fragment; i.e., they call the complex a 16e system.<sup>16</sup> What we found was that the system converged nicely to an  $\eta^2$ - $\text{BH}_4$  (see Supporting Information). Interestingly, as expected for scandium(III) relative to scandium(I), the energy level diagrams (Figure 5b) are reflective of a large HOMO-LUMO gap, essentially double the value obtained for  $\text{Sc}(\text{BrMgL})_2\text{Br}$ . Also, while the symmetry of  $\text{Cp}_2\text{Sc}(\text{BH}_4)$  is low consistent with an expectation of rhombic magnetic

symmetry about Sc, we find instead that  $\delta_{22} \approx \delta_{33}$ , such that the system is (accidentally) nearly axial about  $z$ . The magnetic operator of  $R_z$  symmetry permits strong mixing between HOMO - 3 and LUMO + 2, on one hand, and between HOMO - 2 and LUMO + 1 on the other. Respectively, these orbitals are strong in scandium  $d_{x^2-y^2}$ ,  $d_{xy}$  and  $d_{xz}$ ,  $d_{yz}$  character (see Supporting Information). The HOMO for  $\text{Cp}_2\text{Sc}(\text{BH}_4)$  is quite delocalized, involving metal-ring  $\pi$  bonding as well as terminal B-H bonding. The LUMO is nearly a pure scandium  $d_z^2$  orbital consistent with assignment of this molecule as a Lewis acidic 16e complex. This orbital plays a role in the strongest occupied-virtual mixings associated with  $\delta_{22}$  and  $\delta_{33}$  (see Supporting Information). Having discussed the magnetic anisotropy associated with the two scandium systems considered here, as well as the underlying molecular orbital basis for the anisotropy, we turn attention now to the total isotropic shielding for these systems. The compound  $\text{Cp}_2\text{Sc}(\text{BH}_4)$  has been reported to have an isotropic solution  $^{45}\text{Sc}$  NMR shift in  $\text{C}_6\text{D}_6$  of +67.5 ppm relative to saturated  $\text{ScCl}_3$  in  $\text{D}_2\text{O}$ . Taking  $\text{Cp}_2\text{Sc}(\text{BH}_4)$  as our reference compound, we can convert a given calculated shielding value  $\sigma(\text{calc})$  into a chemical shift  $\delta$  via the equation:  $\delta(\text{calc}) = \delta(\text{ref, calc}) - \delta(\text{calc}) + 67$  ppm. The expectation is that  $\text{Sc}(\text{BrMgL})_2\text{Br}$  should exhibit its  $^{45}\text{Sc}$  NMR signal ca. 40 ppm downfield relative to  $\text{Cp}_2\text{Sc}(\text{BH}_4)$ . On the other hand, the compound  $\text{Sc}(\text{BrMgL})_2\text{Br}$  ( $\text{L} = (\text{R}_2\text{NCH}_2\text{CH}_2\text{NCMe})_2\text{CH}$ ,  $\text{R} = \text{Et}$ ) has been reported to resonate at  $\delta = 167.5$  ppm relative to  $[\text{Sc}(\text{H}_2\text{O})_6]^{3+}$ ,<sup>7</sup> presumably the same reference used in the case of  $\text{Cp}_2\text{Sc}(\text{BH}_4)$ . The discrepancy between the calculated and observed  $\delta_{\text{iso}}$  is rather substantial, given that the  $^{45}\text{Sc}$  chemical shift range has been estimated to be only ca. 340 ppm.<sup>17</sup> One possible explanation is that the experimental

(17) Kirakosyan, G. A.; Tarasov, V. P.; Buslaev, Yu. A. *Magn. Reson. Chem.* **1989**, *27*, 103-111.

## Scheme 2



reference samples used might possibly differ in their chemical shifts; the pH of the aqueous scandium solutions was not stated in either case. A recent  $^{45}\text{Sc}$  NMR study reported the use of  $\text{Sc}(\text{NO}_3)_3$  in water at pH 1 as the reference standard.<sup>18</sup> On the other hand, Schreckenbach has pointed out that calculated metal NMR shifts are very sensitive to small changes in structure (i.e., bond lengths) and to the absolute calculated MO energies, both of which can vary according to the specific choice of computational method.<sup>14</sup> Regardless of our ability at present to accurately calculate absolute isotropic NMR shieldings, we assert that the type of study carried out here has great value in being able to relate the anisotropy of the magnetic shielding to the molecular electronic structure. We expect that the gross features of the anisotropy should be relatively independent of the computational method employed, and accordingly propose that solid-state  $^{45}\text{Sc}$  NMR may be the best method firmly to connect the molecular orbitals discussed herein to the NMR observable.<sup>19</sup>

The foregoing discussion substantiates the formal oxidation state of +1 for Sc in complex **1**, while recognizing that the phenomenon of  $\delta$  back-bonding to the LMgBr ring LUMOs draws some of electron density away from Sc. It is difficult to conceive a reaction complex **1** might undergo in which scandium maintains its unusual oxidation state(I).<sup>19</sup> This is because the disposition and the electronic configuration of LMgBr have a decisive contribution to the stability of complex **1**. Attempts to exchange LMgBr for other ligands were not successful. Accordingly, investigation of the reactivity of **1** has proceeded in the direction of redox reactions with substrates possessing acidic hydrogens, including alcohols and water.

**Reaction of 1 with the Water Adduct  $\text{H}_2\text{O} \cdot \text{B}(\text{C}_6\text{F}_5)_3$ .** For a controlled hydrolysis,  $\text{H}_2\text{O} \cdot \text{B}(\text{C}_6\text{F}_5)_3$  was used, and product **2** was isolated (Scheme 2). The volatiles of this reaction were analyzed by GC-MS, and  $\text{C}_6\text{F}_5\text{H}$  was identified as a byproduct (Scheme 2).

With these findings, we can propose a path involving the reduction of water by scandium, which in turn is oxidized to the (3+) state. In compensation to the fragmentation of molecule **1**, the ligand (L) migrates for stabilizing the oxidized scandium, and the  $\text{B}(\text{C}_6\text{F}_5)_3$  molecule is cleaved.<sup>20</sup> In compound **2**, scandium adopts a pseudo-octahedral geometry ( $\text{O}(1)\text{---Sc---O}(2)$   $166.1^\circ$ ) forming a perfect planar

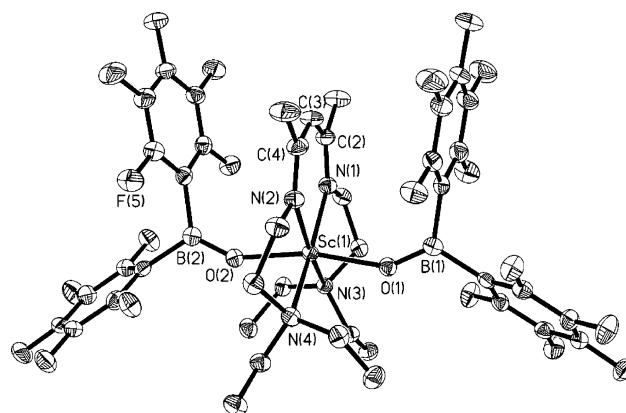


**Figure 6.** Molecular structure of **2**. Solvent and protons are omitted for clarity.

**Table 2.** Selected Bond Distances (Å) and Angles (deg) for **2**

bond lengths		angles	
C(1)–C(2)	1.508(4)	O(1)–Sc–O(2)	166.1(7)
C(4)–C(5)	1.521(4)	C(2)–C(3)–C(4)	129.5(2)
C(2)–C(3)	1.402(4)	Sc(1)–O(1)–B(1)	145.84(17)
N(1)–C(2)	1.331(3)	Sc(1)–O(2)–B(2)	149.90(17)
B(1)–O(1)	1.296(3)	N(1)–Sc(1)–N(2)	85.33(8)
B(2)–O(2)	1.290(3)	N(1)–C(2)–C(3)	123.9(2)
Sc(1)–O(1)	2.0449(17)	N(2)–C(4)–C(3)	124.1(2)
Sc(1)–O(2)	2.0481(17)	N(1)–Sc(1)–N(3)	79.15(8)
Sc(1)–N(1)	2.163(2)	N(2)–Sc(1)–N(4)	79.15(8)
Sc(1)–N(2)	2.171(2)	N(3)–Sc(1)–N(4)	116.59(7)
Sc(1)–N(3)	2.402(2)	C(2)–N(1)–Sc(1)	128.53(17)
Sc(1)–N(4)	2.392(2)	C(4)–N(2)–Sc(1)	128.51(18)

six-membered ring with the  $\beta$ -diketiminato backbone (Figure 6). The differences in bond lengths within the  $\beta$ -diketiminato moiety among **1**, **2**, and  $\text{LScBr}_2$ <sup>21</sup> are negligible (C(1)–C(2) 1.411 Å in **1**, 1.401 Å in **2**, and 1.394 Å in  $\text{LScBr}_2$ ; N(1)–C(1) 1.385 Å in **1**, 1.330 Å in **2**, and 1.340 Å in  $\text{LScBr}_2$ ), and the B–O bond length in **2** (av 1.292 Å) is also very close to a covalent B–O bond (1.311 Å),<sup>20</sup> although much shorter than the coordinative B–O bond found in  $\text{H}_2\text{O} \cdot \text{B}(\text{C}_6\text{F}_5)_3$  (1.597 Å)<sup>22</sup> (Table 2). An interesting feature of this structure is the arrangement of two  $\text{C}_6\text{F}_5$  groups almost parallel contiguous to the ScNCCCN ring in **1**. Obviously this has a direct influence on the electron density on the proton from the  $\text{C}(\text{Me})\text{CHC}(\text{Me})$  position whose resonance in the  $^1\text{H}$  NMR spectrum is significantly upfield shifted from 4.82 ppm in  $\text{LScBr}_2$  to 3.51 ppm in **2**. As expected, the crystal packing reveals the incidence of  $\pi$ – $\pi$  stacking interactions between the  $\text{C}_6\text{F}_5$  groups of different molecules.

(18) Hill, N. J.; Levason, W.; Popham, M. C.; Reid, G.; Webster, M. *Polyhedron* **2002**, *21*, 1579–1588.

(19) See ring displacement reactions with participation of Ln(0) compounds in ref 5a.

(20) Splitting of the  $\text{B}(\text{C}_6\text{F}_5)_3$  molecule is not new. See: Neculai, D.; Roesky, H. W.; Neculai, A. M.; Magull, J.; Walfort, B.; Stalke, D. *Angew. Chem.* **2002**, *114*, 4470–4471; *Angew. Chem., Int. Ed.* **2002**, *41*, 4294–4295.

(21) Neculai, A. M.; Neculai, D.; Nikiforov, G.; Roesky, H. W.; Magull, J.; Schlicker, C.; Herbst-Irmer, R.; Noltemeyer, M. *Eur. J. Inorg. Chem.* **2003**, 3120–3126.

(22) Bergquist, C.; Bridgewater, B. M.; Harlan, C. J.; Norton, K. R.; Friesner, R. A.; Parkin, G. *J. Am. Chem. Soc.* **2000**, *122*, 10581–10590.

Scheme 3

Table 3. Selected Bond Distances (Å) and Angles (deg) for **3** and **1**<sup>a</sup>

compound <b>3</b>				compound <b>1</b>			
Mg–N(1)	2.087(3)	C(2)–C(3)–C(4)	128.0(3)	Mg–N(1)	2.142(2)	C(1)–C(2)–C(4)	129.1(4)
Mg–N(2)	2.094(3)	N(2)–Mg–N(1)	88.22(12)	Mg–N(2)	2.345(2)	N(1)–Mg–N(1)#2	82.14(12)
Mg–N(3)	2.309(3)	N(4)–Mg–N(3)	99.29(11)			N(2)–Mg–N(2)#2	110.62(12)
Mg–N(4)	2.335(3)	N(3)–Mg–N(1)	79.32(11)			N(2)–Mg–N(1)	79.76(8)
C(1)–C(2)	1.532(5)	N(2)–Mg–N(4)	78.87(11)	C(1)–C(3)	1.511(4)		
C(2)–C(3)	1.411(5)			C(1)–C(2)	1.411(3)		
C(2)–N(1)	1.341(5)			C(1)–N(1)	1.385(3)		
C(4)–N(2)	1.334(5)						

<sup>a</sup> Symmetry transformations used to generate equivalent atoms for **1**: #1  $-x, y, z$ ; #2  $x, y, -z + 3/2$ ; #3  $-x, y, -z + 3/2$ .

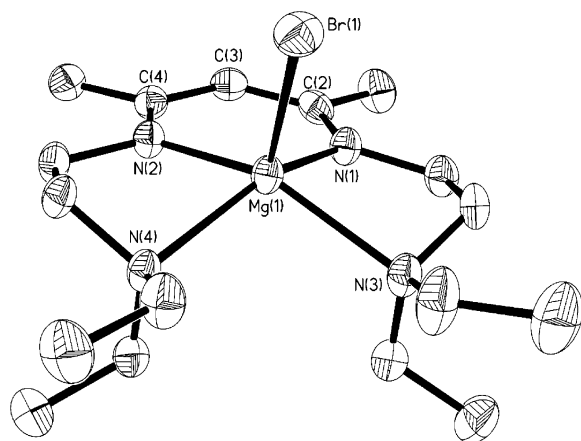


Figure 7. Molecular structure of **3**. Solvent and protons are omitted for clarity.

**Reaction of **1** with (HOCH<sub>2</sub>)<sub>2</sub>CMe<sub>2</sub>; Formation of LMgBr (**3**).** The reduction using alcohols led as expected to the cleavage of the sandwich molecule **1** with isolation only of the protective groups LMgBr (Scheme 3).

The reaction was monitored by <sup>1</sup>H NMR spectroscopy. Because of the complexity of the reaction mixture, only representative resonances were followed. The observations are consistent with a redox reaction; namely, the HOCH<sub>2</sub> resonances fully disappeared from the initial position (2.04 ppm) in the spectrum of the alcohol in the deuterated solvent. The resonance corresponding to the proton from C(Me)CHC–(Me) position was shifted from 2.82 ppm in **1** to 4.74 ppm in the reaction mixture, analogous with the resonance found for the same proton from the final isolated product LMgBr. The characteristic resonances of LMgBr can be found in the final spectrum. A spectral subtraction of the resonances of **3** gave no useful information about the scandium product(s). The only useful information extracted from the <sup>45</sup>Sc NMR spectrum (due to the multiple peaks) was related to the disappearance of the characteristic resonance for complex **1** (167 ppm).

Examination of the bond lengths and angles revealed by the X-ray structure of **3** (Figure 7) is important because it facilitates the understanding of the influence of the coordination of ScBr to the LMgBr molecule.

Moreover, the structure of **3** indicates that during the

transformation L has not changed (preservation of its monoanionic character) (Scheme 1). The pentacoordinated magnesium atom is in a pyramidal environment having the Mg–N bond distances slightly shorter compared to those in **1** (Mg–N( $\beta$ -diketiminato) 2.087 Å; 2.094 Å in **3** and 2.142 Å in **1**; Mg–N(coordinated arms) 2.309 Å, 2.335 Å in **3** and 2.345 Å in **1**) attributable most likely to the higher coordination number of Mg in **1** versus **3**. These values accommodate with the literature data for  $\beta$ -diketiminato magnesium complexes.<sup>23</sup> Furthermore, we were interested in a comparison of distances and angles within the  $\beta$ -diketiminato backbone (C(1)–C(2) in **1** 1.411 Å, C(2)–C(3) 1.411 Å, C(4)–C(3) 1.415 Å in **3**; C(1)–N(1) in **1** 1.385 Å, C(2)–N(1) in **3** 1.341 Å, the internal angle being 129.1° in **1** and 128.03° in **3**). A closer look shows that in fact the dimensions do not change so much to conclude that the LMgBr in **1** is negatively charged (anion or radical-anion). The slightly shorter C–N bonds in **3** compared to **1** can be attributed to the different coordination numbers around the  $\beta$ -diketiminato nitrogen atoms, together with removal of the  $\delta$ -back-bonding understood to be operative in the case of **1** (Table 3).

Note that the deviation of the Mg from the N<sub>2</sub>C<sub>3</sub> plane is significantly lower in **3** (0.22 Å) compared to **1** (1.09 Å). In general, the magnesium ion coordination of L may be understood to be flexible.<sup>24</sup> In compound **1**, the conformation is presumably forced by sandwiching Sc together with repulsive interactions involving the Sc and Mg-bound bromine atoms.

## Conclusion

Herein we have provided computational support for the statement that in compound **1** the formal oxidation state of

- (23) (a) Dove, A. P.; Gibson, V. C.; Hornmirmur, P.; Marshall, E. L.; Segal, J. A.; White, A. J. P.; Williams, D. J. *J. Chem. Soc., Dalton Trans.* **2003**, 3088–3097. (b) Chisholm, M. H.; Gallucci, J.; Phomphrai, K. *Inorg. Chem.* **2002**, *41*, 2785–2794. (c) Chamberlain, B. M.; Cheng, M.; Moore, D. R.; Oviatt, T. M.; Lobkovsky, E. B.; Coates, G. W. *J. Am. Chem. Soc.* **2001**, *123*, 3229–3238. (d) Cheng, M.; Attygalle, A. B.; Lobkovsky, E. B.; Coates, G. W. *J. Am. Chem. Soc.* **1999**, *121*, 11583–11584.
- (24) (a) Randall, D. W.; DeBeer George, S.; Holland, P. L.; Hedman, B.; Hodgson, K. O.; Tolman, W. B.; Solomon, E. L. *J. Am. Chem. Soc.* **2000**, *122*, 11632–11648. (b) Deng, L.; Schmid, R.; Ziegler, T. *Organometallics* **2000**, *19*, 3069–3076.

scandium is +1. The DFT calculations are in good agreement with the experimental data and disclosed that HOMO has substantial Sc  $d_{yz}$  character, but it is additionally delocalized onto the ligands via a  $\delta$  back-bonding mechanism. This delocalization represents stabilization of the unusual +1 oxidation state for scandium. Moreover, although the skeletal arrangement of the molecule was not maintained, redox processes in which **1** was involved helped to understand the chemistry of such a system and are in concert with the initial formulation of **1**. Also the fact that the L ligand was not activated during these reactions lends a bias toward the formulation of the ligand as having consistent monoanionic character.<sup>25</sup> Importantly, the synthetic method for obtaining

compound **1** relies on solution chemistry, thus illustrating an alternative to metal atom vapor methods for preparing low-valent scandium compounds.

**Acknowledgment.** Financial support of the Deutsche Forschungsgemeinschaft is gratefully acknowledged.

**Supporting Information Available:** The CIF files for compounds **2** and **3** and details of the computational study. This material is available free of charge via the Internet at <http://pubs.acs.org>.

IC034947O

---

(25) Eisenstein, O.; Hitchcock, P. B.; Khvostov, A. V.; Lappert, M. F.; Maron, L.; Perrin, L.; Protchenko, A. V. *J. Am. Chem. Soc.* **2003**, *125*, 10790–10791.